

## Comparison of KAERI Results on IAEA CRP Phase4 Benchmark Problem for Liquid Metal Fast Reactor Reactivity Effects

Ki Bog Lee, Jin Wook Jang, Hoon Song and Young Il Kim

Korea Atomic Energy Research Institute  
P.O. Box 150, Yusong-gu, Taejon, 305-600, Korea

### Abstract

IAEA Coordinated Research Project (CRP) proposed a benchmark problem in order to validate, verify and improve methodologies and computer codes used for the calculation of reactivity coefficients in fast reactors aiming at enhancing the utilization of plutonium and minor actinides.

The purpose of this paper is to report the calculation results based on the K-CORE system developed by KAERI and to compare the results performed by the each participant for the IAEA CRP Phase 4 of BN-600 full mixed oxide (MOX) fueled core benchmark analyses. The K-CORE calculational methods employed in the benchmark analyses are explained. The benchmark results carried out by KAERI and the other participants are collected and inter-compared.

According to comparison results, the  $k$ -eff and the fuel Doppler coefficients of KAERI shows a little bit higher than the other's values mainly due to using JEF 2.2 cross section data library. The fuel density coefficients and the effective delayed neutron fraction and the neutron lifetime show good agreement compared with the other participants' values. Even though the KAERI results for the steel Doppler, fuel density and sodium density coefficients, exists in the range of minimum and maximum values between the participants, there are big discrepancies in reactivity coefficients. So the prediction of reactivity coefficients requires further investigation.

### 1. Introduction

The IAEA Coordinated Research Project (CRP) sponsored a meeting entitled "A Updating Codes and Methods to Reduce the Calculational Uncertainties of the Liquid Metal Fast Reactor (LMFR) reactivity Effects" which had held in Vienna on 24-26 November 1999. The general objective of this meeting is to validate, verify and improve methodologies and computer codes used for the calculation of reactivity coefficients in fast reactors aiming at enhancing the utilization of plutonium and minor actinides. As a part of that meeting, a benchmark was proposed so that differing analysis groups could compare calculational methodologies and various calculated parameters for a specific loading configuration. The

configuration chosen, following a proposal by the Russian Federation, was a hybrid BN-600 reactor configuration which has a combination of low enriched uranium (LEU), middle enriched uranium (MEU), high enriched uranium (HEU) and mixed oxide assemblies in the core region. Later, as a follow-up to this hybrid benchmark, a full mixed oxide fuel benchmark so called Phase 4 model was also proposed. Thus the benchmark clearly pursues the utilization of weapons-grade plutonium for energy production in a mixed UOX/MOX or full MOX core of the BN-600 reactor.

Nine organizations from eight member states and one from the IAEA participated in the hybrid BN-600 core benchmark analyses. The benchmark analyses consist of three Phases during 1999 - 2001; RZ homogeneous benchmark (Phase 1), Hex-Z homogeneous benchmark (Phase 2), and Hex-Z heterogeneous and burnup benchmark (Phase 3). Also the Hex-Z homogeneous full MOX core benchmark model (Phase 4) is being performed during 2002-2003. The participants applied their own current-state-of-basic data, computer codes and methods to the benchmark analyses. The results obtained by the participants for each Phase were inter-compared in terms of calculational uncertainty and evaluated their effects on the core transient behaviour.

In the Phase 1 and 2 studies, the input data including RZ and Hex-Z calculational models for the BN-600 benchmark calculations were completely described in the benchmark definitions [1,2]. The calculational model of the BN-600 reactor corresponds to the reactor of total power 1470 MW<sub>th</sub> at the beginning of an equilibrium cycle, when the impact of the control rods is the strongest. The core consists of a low enrichment inner zone (LEZ), a middle enrichment zone (MEZ) and a high enrichment outer zone (HEZ). Between MEZ and HEZ a mixed oxide zone is located. Three control rod zones and one scram rod zone are radially inter-dispersed in LEZ. The outer core zone is bounded by two steel shielding zones, followed by a radial reflector zone. Total twelve parameters for integral value and/or its spatial distribution were calculated for the RZ and Hex-Z calculational models by diffusion and transport theory methods, using homogeneous representations of the material regions. Spatial distributions of several reactivity coefficients were obtained by first order perturbation theory method. The core power distribution was normalized to a total power of 1470 MW assuming energy is deposited at its point of fission with an energy of 200 MeV per fission and 0 MeV per capture for all nuclides.

Phase 3 calculations were performed by diffusion and transport theory methods for the Hex-Z model only. For the burnup analysis a single stage calculation has been assumed with no recalculation of the flux or resonance self-shielding for sub time steps. The burnup period is 140 effective full power days at an assumed 100 % load factor. To evaluate the heterogeneity effect and the burnup effect,  $k_{\text{eff}}$ , fuel Doppler coefficient and sodium density coefficient were mainly calculated at the beginning of cycle (BOC) and the end of cycle (EOC) for both homogeneous and heterogeneous core models. A heterogeneous treatment has been applied to the core fuel regions and the control rods in heterogeneity calculations. The control rod worth at BOC and the reactivity loss with burnup were also evaluated.

The inter-comparison of the results for Phase 1 and 2 obtained by the homogeneous representation shows good agreement in most parameters. But in the inter-comparison of the Phase 3 results, the heterogeneity effect on  $k_{\text{eff}}$  and control rod worth appeared to differ depending on the heterogeneity treatment method. It is generally recognized that it is important to investigate the power distribution in the MOX fuelled region in association with reaction rates distributions in order to comprehend the uncertainties in reactivity coefficients. The results of previous Phases 1 through 3 are compared with each other and documented in References [1]-[3].

The purpose of this paper is to report the calculation results based on the KAERI's K-CORE system and to compare the results performed by the each participant for the Phase 4 of

BN-600 full MOX fueled core benchmark analyses. In following section 2, the The BN-600 full MOX core model (Phase 4) based on the specification in Reference[4] is described in details. The K-CORE calculational methods employed in the benchmark analyses are explained in section 3. The benchmark results carried out by KAERI and the other participants are collected and inter-compared in section 4.

## 2. Benchmark Description

### 2.1 Homogeneous benchmark model

A 60° sector of the layout of the benchmark core model is shown in Fig.1. In principle, the core layout is the same as that of the previous benchmark hybrid core of BN-600 [3]. The same geometry descriptions for fuel subassemblies (FSAs) and control rods have been retained in a trigonal lattice of the same pitch. The same simplifications (60° symmetry and exclusion of automatic compensators) are given. It is seen that, for this benchmark configuration, each enriched region has a burnup of 2-3%, while the internal breeding region (IBZ), which contains relatively more U-238, has a burnup of 1.7%. Interspersed radially in the LEZ zone were three control rod zones (SHR) and one scram rod zone (SCR). Radially, beyond the HEU outer driver zone were two steel shielding zones (SSA1 and SSA2) followed by a radial reflector zone (REF).

Compared with the hybrid core model defined in previous benchmark studies, several design modifications have been made in the full MOX core model to preserve the outcome of the benchmark core model. A sodium plenum is located above the core to reduce sodium void effect. An internal breeding zone is inserted in the core mid-plane to achieve the reduction of sodium void effect as sought in the BN-800 core design investigations. To compensate the reduction of core volume resulted from these design changes, an extra row of FSAs is added in MEZ.

All fuel isotopes are modelled at a uniform temperature of 1500 K, and all structural and coolant isotopes are at a uniform temperature of 600 K. Batch-averaged compositions are used and the heterogeneous structure of the core subassemblies has been ignored.

The arrangement of the compositions and cell heights for each cell are indicated in Fig. 2.

### 2.2 Benchmark calculations

Parameters for the benchmark calculation in Phase 4 will be calculated with the control rods insertion as shown in Fig. 2 and will consist of:

- Fuel and steel Doppler coefficients and their distributions;
- Fuel density coefficient and its distribution;
- Sodium density coefficient and its distribution;
- Power distribution for fuel and non-fuelled regions;
- Beta-effective and prompt neutron lifetime.

The definition of the above coefficients is the same as in previous phases of the CRP and introduced in the followings.

#### Fuel Doppler Coefficient

The fuel Doppler coefficient will be calculated for the homogeneous core model for a change in fuel temperature from 1500 K ( $T_1$ ) to 2100 K ( $T_2$ ). Fuel isotopes consist of U235, U236, U238, Pu239, Pu240, Pu241, Pu242, O16 and the average fission product (FP). The

fuel Doppler coefficient is defined as :

$$K_D^{fuel} = \frac{k_{eff}^2 - k_{eff}^1}{k_{eff}^2 k_{eff}^1} \frac{1}{\ln(T_2/T_1)}$$

### **Steel Doppler Coefficient**

The steel Doppler coefficient will be calculated for the homogeneous core model for a change in steel temperature from 600 K ( $T_1$ ) to 900 K ( $T_2$ ). Steel isotopes consist of Fe54, Fe56, Fe57, Fe58, Cr50, Cr52, Cr53, Cr54, Ni58, Ni60, Ni61, Ni62, Ni64 and Mo. The steel Doppler coefficient is defined as :

$$K_D^{steel} = \frac{k_{eff}^2 - k_{eff}^1}{k_{eff}^2 k_{eff}^1} \frac{1}{\ln(T_2/T_1)}$$

### **Fuel Density Coefficient**

The fuel density coefficient will be calculated for the homogeneous model for a 1% increase in fuel density in all zones, and is defined as the reactivity change per unit change in material density :

$$W_{fuel} = \frac{dk}{dr_{fuel}} \frac{r_{fuel}}{k^2}$$

Fuel isotopes consist of U235, U236, U238, Pu239, Pu240, Pu241, Pu242, O16 and FP.

### **Sodium Density Coefficient**

The sodium density coefficient will be calculated for the homogeneous model for a 1% increase in sodium density in all zones, and is defined as:

$$W_{Na} = \frac{dk}{dr_{Na}} \frac{r_{Na}}{k^2}$$

The above parameters have been calculated by all participants using homogeneous representations of the material regions defined in section 2.1 and diffusion theory. Where possible heterogeneous geometry diffusion/transport theory will be optionally used for the calculation of distributed reactivity effects and again optionally heterogeneous transport theory for integral reactor results; it is expected that the presence of the sodium plenum will make heterogeneity and transport effects important.

### **Power Distribution**

Spatially-dependent powers were determined for this model assuming a 200 MeV/fission value with no energy deposition for a capture event, 0 MeV/capture and were normalized to the total 1470 MWt. So the gamma heating (i.e., local energy deposition model) was excluded. This effect is not significant in the core regions, where fission dominates the energy deposition, but can be large in non-fueled regions.

## **3. Calculational methods of KAERI K-CORE System**

All the calculation procedure and evaluation were performed by using the K-CORE System of KAERI. Fig. 3 shows the calculation flow and the connection of codes in the K-CORE system. Based on the self-shielding f-factor approach, the microscopic cross sections

for the benchmark model were generated. An 80-group neutron cross section library, KAFAX(KAERI FAsT XS)/F22 [5] was prepared in the MATXS library format based on the JEF-2.2 nuclear data. This version contains infinite dilute cross sections for various temperatures and Bondarenko self-shielding f-factors. The composition-dependent, 9-group microscopic cross section sets for all reactor constituent materials were generated from KAFAX/F22 at the specified temperatures (1500 K and 2100 K for fuel isotopes including fission product and oxygen, 600 K and 900 K for structural and coolant isotopes) by utilizing the effective cross section generation module composed of TRANSX [6] and TWODANT [7] codes. The data processing in this module includes resonance and spatial self-shielding corrections, reactor and cell flux solutions and cross section group collapsing. Neutron spectra necessary for group collapsing were obtained from the  $P_3S_8$  transport theory calculations for the two dimensional, coarse meshed RZ model for the reference configuration with the TWODANT code. The TWODANT code employing discrete ordinates approximation was used for two-dimensional (RZ) model calculations. The 9-group structure has 1.2 and 1.5 lethargies for the first two energy groups, and a 1.0 lethargy for the remaining 7 energy groups, with the highest energy boundary of 20.0 MeV. The 9-group cross section sets are collapsed from the 80-group structures and the 9-group cross section set is used for all neutronics calculations.

The lumped Pu239 fission product cross sections was generated by collapsing into 9 groups from the cross section library for 172 fission product isotopes of Pu239, fission yields, and a typical neutron spectrum of fuel region of BN-600 full MOX core from TWODANT result as a weighting spectrum.

The neutron multiplication factor  $k_{\text{eff}}$  and basic neutronics parameters such as forward and adjoint neutron flux distribution, power distribution were calculated by using DIF3D [8] associated with the 9-group cross section set. The DIF3D code employs the coarse-mesh nodal diffusion approximation to the Hex-Z geometry model.

Various reactivity parameters such as fuel density coefficients and sodium density coefficients, were calculated by using the PERT-K code [9]. The PERT-K code solves the first order perturbation theory equations based on diffusion theory nodal expansion method using the forward and adjoint flux solutions obtained from DIF3D calculations.

The power distribution for fuel and non-fuelled regions is determined by the energy deposition of fission and capture reactions including the energy deposition of structure and coolant materials capture reactions. These energy deposition values implicitly assumed that the energy generated by fission and capture reactions is deposited at the site of the reaction. However, assuming all core power comes from the fission energy deposition, the powers for non-fuelled region is completely ignored and the core power is normalized for fuel regions only.

The effective delayed neutron fraction,  $\beta_{\text{eff}}$  and the prompt neutron life time were calculated by using the BETA-K code [10]. The BETA-K code can generate several kinetic parameters such as the effective delayed neutron fraction, prompt neutron lifetime, fission spectrum and fission yield data for each fissionable isotope, fuel compositions and the whole core, utilizing the DIF3D forward and adjoint flux solutions. For this calculation, the delayed neutron data such as yield numbers for 6 delayed neutron groups were prepared from the ENDF/B-VI file.

#### 4. Benchmark results

Table 1 shows the eigenvalues of nominal condition and the whole core reactivity coefficients by the whole core direct calculation and the summation of local coefficients for all core regions. In table 1, the direct calculation means that the reactivity coefficient is

computed with the constant cross sections corresponding to the whole core conditions. So the fuel Doppler coefficient for the whole core direct calculation, for example, is determined with the effective multiplication factors(k-eff) at the nominal core condition and the core condition of 2100 K fuel temperature and 600 K structure material temperature. Also the reactivity summation is displayed in Table 1, which is the summation of each region reactivity coefficient for all core regions determined by the local changes. It is noted that the fuel density and sodium density coefficients for local regions were calculated using the first order perturbation theory. The k-eff and the fuel Doppler coefficients of KAERI shows a little bit higher than the other's values. We think this result comes mainly from using the base XS data, JEF2.2 because the k-eff of JEF2.2 is larger than that of JENDL-3.2 by 0.6% dk according to the sensitivity analysis [11] and the similar result is reported in Reference [12]. The fuel density coefficients and the effective delayed neutron fraction and the neutron lifetime displayed in Table 2, show good agreement compared with the other's values. But the sodium density coefficient shows big discrepancies between the participants, not even the sign is same. The sodium density coefficient is sensitive and affected by axial and radial leakage due to the flux distribution. So the prediction of the sodium density coefficients requires further investigation in the view point of flux distribution due to various effects, such as leakage treatment method, neutron grouping, boundary condition etc.

The KAERI result of power distribution is observed in Table 3 and the power of the specified regions are compared in Table 4. When it is assumed that there is no energy deposition for a pure capture event, 98.0% of the power is in the enriched region and 2.0% is in the axial blanket region. The KAERI and FZK results show bigger values in the axial blanket region but the enriched zonewise power shows good agreement for all participants.

## 5. Conclusion

In this paper, the procedure and method for liquid metal fast reactor reactivity coefficients by the K-CORE system is introduced and the comparison of KAERI results with the other participants' results for the IAEA CRP Phase 4 benchmark problem is carried out. The k-eff and the fuel Doppler coefficients of KAERI shows a little bit higher than the other's values mainly due to using JEF 2.2 cross section data library. The fuel density coefficients and the effective delayed neutron fraction and the neutron lifetime show good agreement compared with the other participants' values. Even though the KAERI results for the steel Doppler, fuel density and sodium density coefficients, exists in the range of minimum and maximum values between the participants, there are big discrepancies in reactivity coefficients. So the prediction of reactivity coefficients requires further investigation in the view point of flux distribution due to various effects, such as leakage treatment method, neutron grouping, boundary condition etc.

## 6. Acknowledgement

This study has been carried out under the Nuclear R&D Program sponsored by the Ministry of Science and Technology of Korea and International Atomic Energy Agency.

## 7. References

- [1] "Working Material: Updated Codes and Methods to Reduce the Computational Uncertainties of the LMFR Reactivity Effects, First Research Co-ordination Meeting," Vienna, 24-26 November

- 1999, IAEA-RC-803, IWGFR/100.
- [2] “Working Material: Updated Codes and Methods to Reduce the Calculational Uncertainties of the LMFR Reactivity Effects, Second Research Co-ordination Meeting,” Vienna, 24-26 November 2000, IAEA-RC-803.2, IWG-FR/103.
  - [3] “Working Material: Updated Codes and Methods to Reduce the Calculational Uncertainties of the LMFR Reactivity Effects, Third Research Co-ordination Meeting,” Cadarache, 12-16 November 2001, IAEA-RC-803.3, IWGFR/106.
  - [4] V. Y. Stogov et als., “Specification of Phase 4 Benchmark (Hex-Z Fully Fuelled Core Model of BN-600)(Rev. 3.1),” IPPE, received from a IAEA organizer [Young-In.Kim@iaea.org](mailto:Young-In.Kim@iaea.org), (2002).
  - [5] J. D. Kim and C. S. Gil, “KAFAX-F22: Development and Benchmark of Multi-group Library for Fast Reactor Using JEF-2.2,” KAERI/TR-842/97, KAERI (1997).
  - [6] R. E. MacFarlane, “TRANSX 2: A Code for Interfacing MATXS Cross-Section Libraries to Nuclear Transport Codes,” LA-12312-MS, LANL (Dec. 1993).
  - [7] R. E. Alcouffe, et als., “User’s Guide for TWODANT: A Code Package for Two-Dimensional, Diffusion-Accelerated, Neutron Transport,” LA-10049-M, LANL.(Feb. 1990).
  - [8] K. L. Derstine, “DIF3D: A Code to Solve One-, Two-, and Three-Dimensional Finite-Difference Difference Diffusion Theory Problems,” ANL-82-64, ANL (April 1984).
  - [9] T. K. Kim, et als., “Development of A Perturbation Code, PERT-K, for Hexagonal Core Geometry,” KAERI/TR-1194/98, KAERI (1998).
  - [10] T. K. Kim, et als., “Development of An Effective Delayed Neutron Fraction Calculation Code, BETA-K,” KAERI/TR-1120/98, KAERI (1998).
  - [11] Makoto Ishikawa, “Sensitivity Analysis of JEF and JENDL (Action 3.6),” The document of O-arai Engineering Center, JNC (May 2002).
  - [12] Wacław Gudowski, et. als., “IAEA Benchmark on Accelerator-Driven Systems,” to be published.

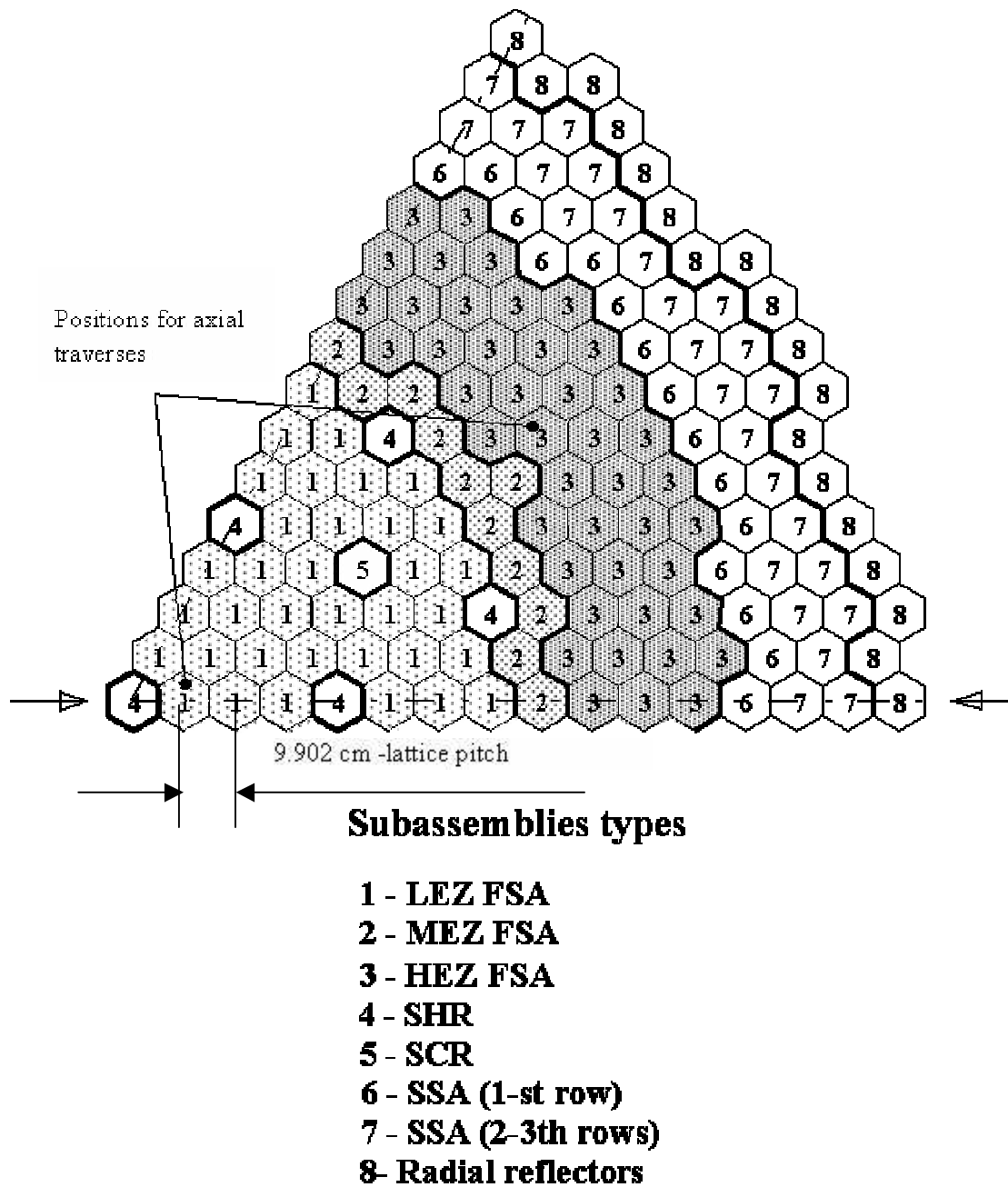


Figure 1. Layout of full MOX BN-600 model (60° sector, rotational symmetry)

	dZ cm	dZ cm		LEZ	MEZ	HEZ	SHR	SCR	SSA1	SSA2, 3	Radial Reflector
		for output		1	2	3	4	5	6	7	8
Reflector	30.0	30.0		22	22	22	22	22	22	22	21
Cones	4.5	4.5		12	12	12	14	16	19	20	21
Upper Boron Shield	15.0	5.0		13	13	13	14	16 SCR	19	20	21
		5.0									
		5.0									
Cones	4.5	4.5		12	12	12	14	17	19	20	21
Sodium Plenum	23.0	8.0		11	11	11	14	17	19	20	21
		8.0									
		7.0									
Plugs	5.3	5.3		10	10	10	14	17	19	20	21
Core	41.15	8.23		1 LEZ	2 MEZ	3 HEZ	14 SHR	17	19 SSA1	20 SSA2, 3	21 Radial Reflector
		8.23									
		8.23									
		8.23									
		8.23									
Internal Breeding Zone	5.1	5.1		23 IBZ	2	3	15	18	19	20	21
Core	41.15	8.23		1 LEZ	2 MEZ	3 HEZ	15	18	19 SSA1	20 SSA2, 3	21 Radial Reflector
		8.23									
		8.23									
		8.23									
		8.23									
Axial Blanket 1	5.5	5.5		7	8	9	15	18	19	20	21
Axial Blanket 2	29.7	9.7		4	5	6	15	18	19	20	21
		10.0									
		10.0									
Reflector	30.0	30.0		22	22	22	22	22	22	22	21

Figure 2. Arrangement of the compositions and cell heights of the full MOX core model of BN-600

**Table 1 Results of Reactivity Coefficients (Homogeneous Diffusion Theory)**

Item	Cal. Method	$(\Delta k/k' / \Delta \ln K)$ or $(\Delta k/k') / (\Delta \bar{n} / \bar{n})$							
		KAERI Korea	IPPE Russia	CIAE China	ANL USA	FZK Germany	JNC Japan	J-EU EU	IGCAR India
	XS Data	JEF2.2	ABBN-93	ENDF/B-VI CENDL-2	ENDF/B-V.2	JENDL-3.2 ENDF/B-6.7	JENDL-3.2	JEF2.2	XSET-98
N. Energy Groups	9	18	12	230	26	18	33	26	
Reference Value (Fuel: 1500K, Steel: 600K)	Keff	1.00976	0.99508	0.98834	1.00374	1.00254	0.99701	1.00183	1.00164
Fuel Doppler (Fuel: 2100K, Steel: 600K)	Direct Cal.	-8.88E-03		-6.83E-03		-6.37E-03	-7.64E-03	-7.90E-03	
	Sum of Local	-8.95E-03	6.84E-03	-7.06E-03	-7.10E-03	-6.52E-03	-7.67E-03	-7.90E-03	-7.73E-03
Steel Doppler (Fuel: 1500K, Steel: 900K)	Direct Cal.	-1.01E-03		-7.24E-04		-5.15E-04	-9.68E-04	-1.24E-03	
	Sum of Local	-1.01E-03	-1.10E-03	-1.13E-03	-7.90E-04	-5.12E-04	-9.72E-04	-1.24E-03	
Fuel Density 1% Change (Fuel Density*1.01)	Direct Cal.	3.72E-01		3.91E-01		3.88E-01	3.95E-01	3.88E-01	
	Sum of Local *	3.80E-01	3.83E-01	3.84E-01	3.55E-01	3.89E-01	3.79E-01	3.88E-01	3.89E-01
Sodium Density 1% Change (Sodium Density*1.01)	Direct Cal.	2.23E-03		-9.87E-04		2.98E-03	3.02E-03	-1.99E-03	
	Sum of Local *	4.75E-04	1.98E-03	-1.70E-03	1.35E-02	1.27E-03	3.40E-03	-1.77E-03	-6.55E-03

\* First Order Perturbation Theory Calculation

**Table 2 Comparison of Beta-effective and Prompt Neutron Lifetime**

Item	KAERI Korea	IPPE Russia	CIAE China	ANL USA	FZK Germany	JNC Japan	J-EU EU	IGCAR India
Effective Delayed Neutron Fraction	3.42E-03	3.44E-03	3.48E-03	3.24E-03	3.34E-03	3.36E-03	3.50E-03	3.46E-03
Neutron Lifetime (sec)	4.26E-07	4.53E-07	4.09E-07	4.11E-07	4.13E-07	4.48E-07	4.36E-07	4.51E-07

**Table 3 KAERI Result of Power Distribution for Fuel Regions (Fission Power only)**

[Unit: watts]

	Height (cm)	dZ (cm)	Region ID	LEZ 1	MEZ 2	HEZ 3
Core	152.60	8.23	P	3.181E+07	1.147E+07	4.322E+07
	144.37	8.23	O	3.992E+07	1.461E+07	5.337E+07
	136.14	8.23	N	4.781E+07	1.762E+07	6.354E+07
	127.91	8.23	M	5.443E+07	2.014E+07	7.184E+07
	119.68	8.23	L	5.953E+07	2.209E+07	7.750E+07
Internal Breeding Zone Core	111.45	5.10	K	1.812E+07	1.440E+07	4.951E+07
	106.35	8.23	J	6.458E+07	2.365E+07	7.988E+07
	98.12	8.23	I	6.401E+07	2.305E+07	7.670E+07
	89.89	8.23	H	5.990E+07	2.125E+07	6.997E+07
	81.66	8.23	G	5.266E+07	1.840E+07	6.011E+07
	73.43	8.23	F	4.314E+07	1.483E+07	4.815E+07
(sum of Core)				5.359E+08	2.015E+08	6.938E+08
Axial Blanket 1	65.20	5.50	E	6.097E+06	1.836E+06	5.084E+06
Axial Blanket 2	59.70	9.70	D	6.255E+06	1.833E+06	5.056E+06
	50.00	10.00	C	3.873E+06	1.085E+06	2.947E+06
	40.00	10.00	B	2.365E+06	6.375E+05	1.736E+06
(sum of AB2)				1.249E+07	3.556E+06	9.738E+06
(sum of AB)				1.859E+07	5.392E+06	1.482E+07
(sum)				5.545E+08	2.069E+08	7.086E+08
Total Power				1.470E+09		

**Table 4 Comparison of Local Power Distribution**

Total Fission Power = 1.470E+09 MWt

Region ID	KAERI Korea	IPPE Russia	CIAE China	ANL USA	FZK Germany	JNC Japan	J-EU EU	IGCAR India
LEZ-D	6.255E+06		4.964E+06	4.660E+06	6.525E+06	5.056E+06	5.171E+06	4.974E+06
LEZ-F	4.314E+07		4.305E+07	4.070E+07	4.544E+07	4.292E+07	4.286E+07	4.237E+07
LEZ-K	1.812E+07		1.741E+07	1.660E+07	1.900E+07	1.778E+07	1.751E+07	1.709E+07
LEZ-P	3.181E+07		3.148E+07	3.150E+07	3.255E+07	3.433E+07	3.164E+07	3.160E+07
MEZ-D	1.833E+06		1.561E+06	1.400E+06	1.875E+06	1.477E+06	1.534E+06	1.472E+06
MEZ-F	1.483E+07		1.498E+07	1.460E+07	1.526E+07	1.478E+07	1.493E+07	1.492E+07
MEZ-K	1.440E+07		1.460E+07	1.440E+07	1.461E+07	1.454E+07	1.443E+07	1.440E+07
MEZ-P	1.147E+07		1.146E+07	1.180E+07	1.140E+07	1.223E+07	1.166E+07	1.166E+07
HEZ-D	5.056E+06		4.490E+06	3.840E+06	4.919E+06	3.954E+06	4.176E+06	4.045E+06
HEZ-F	4.815E+07		4.850E+07	4.910E+07	4.705E+07	4.732E+07	4.902E+07	4.963E+07
HEZ-K	4.951E+07		4.980E+07	5.200E+07	4.768E+07	4.915E+07	5.017E+07	5.071E+07
HEZ-P	4.322E+07		4.277E+07	4.550E+07	4.073E+07	4.437E+07	4.478E+07	4.473E+07
Sum of LEZ	5.545E+08		5.507E+08	5.127E+08	5.775E+08	5.593E+08	5.452E+08	5.390E+08
Sum of MEZ	2.069E+08		2.087E+08	2.023E+08	2.100E+08	2.088E+08	2.070E+08	2.066E+08
Sum of HEZ	7.086E+08		7.105E+08	7.251E+08	6.825E+08	7.019E+08	7.177E+08	7.244E+08
Sum of Core	1.431E+09		1.437E+09	1.440E+09	1.431E+09	1.438E+09	1.438E+09	1.438E+09
Sum of AB	3.881E+07		3.318E+07	2.989E+07	3.929E+07	3.157E+07	3.221E+07	3.202E+07

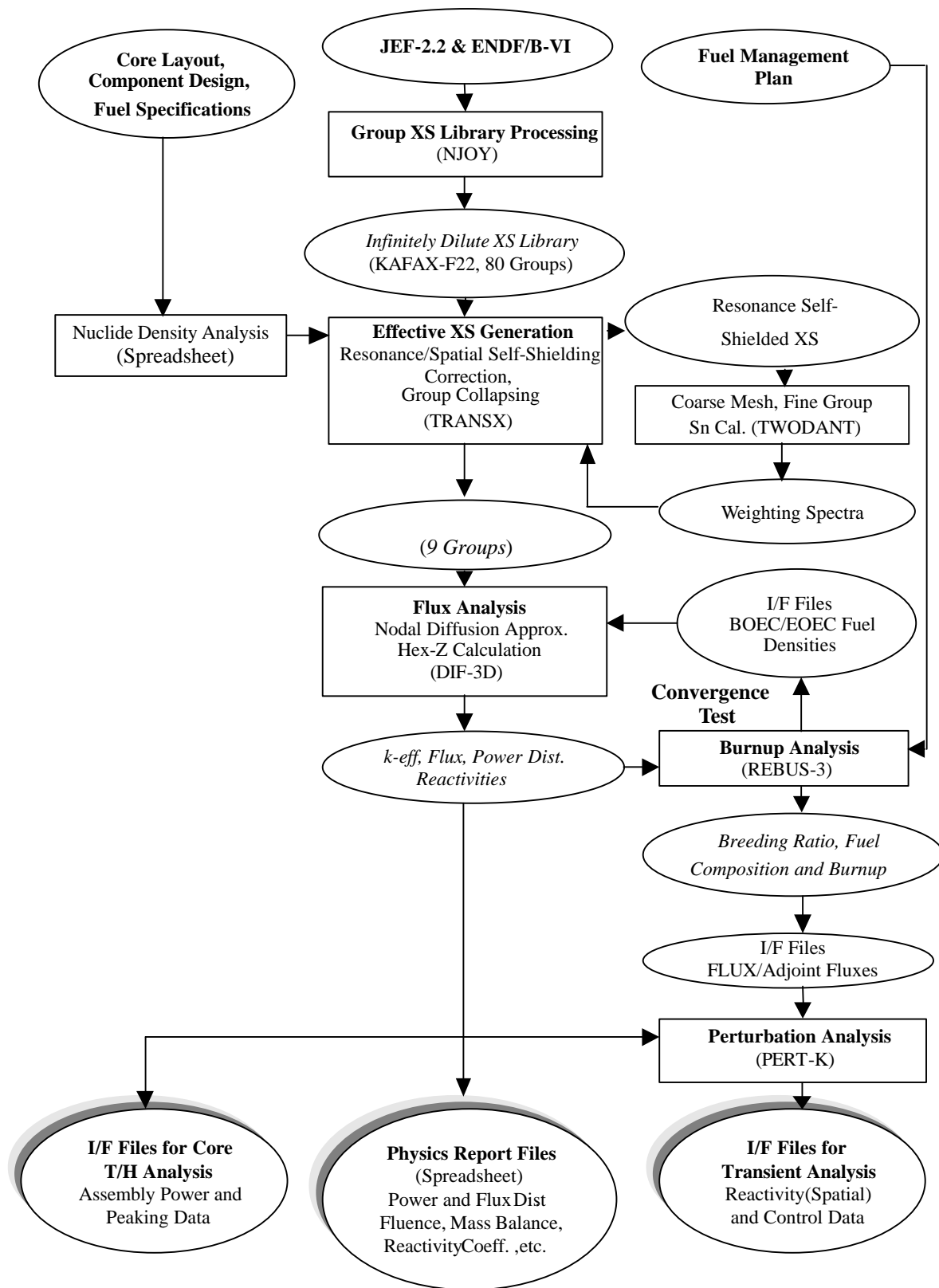


Figure 3. K-CORE System